

# Time Domain Planar Near Field Measurement Simulation

SHEN XianJun

East China Research Institute of Electronic Engineering, Hefei 230031, China  
Dept . of Electronic Engineering and Information Science , Anhui University , Hefei 230039, China

CHEN Xu

East China Research Institute of Electronic Engineering , Hefei 230031, China

## ABSTRACT

The UWB radar operates simultaneously over large bandwidth and the antenna parameters must refer to simultaneous performance over the whole of the bandwidth. Conventional frequency domain (FD) parameters like pattern, gain, etc. are not adequate for UWB antenna. This paper describes an UWB radar antenna planar near field (PNF) measurement system under construction to get the impulse response or transient characteristic of the UWB antenna. Unlike the conventional antenna or RCS time domain test system, the UWB radar signal instead of the carrier-free short time pulse was used to excite the antenna that can avoid the decrease of the dynamic range and satisfy the needs of SAR and the other UWB radar antennas measurement. In order to demonstrate the data analysis program, FDTD simulation software was used to calculate the E-field of  $M \times N$  points in a fictitious plane at different times just like the actual oscilloscope's sampling signals in the time domain planar near field (TDPNF) measurement. The calculated results can be considered the actual oscilloscope's sampling output signals. Through non-direct frequency domain near field to far field transform and direct time domain near field to far field transform, we get the almost same radiation patterns comparing to the FD measurements and software simulation results. At last, varied time windows were used to remove the influences of the non-ideal measurement environment.

**Keywords:** Measurement System, Time Domain, Planar Near Field, UWB Signal, Simulation, Fast Fourier Transform, Finite-Difference Time-Domain

## 1.0 Introduction

In recent years, the ultra-wide band (UWB) antennas have many applications in communication and radar systems such as SAR(Synthetic Aperture Radar) or GPR(Ground Penetrating Radar) with broad-band and fine spatial resolution features. The UWB performances of antennas are resulted in the most practical cases from excitation by impulse or non-sinusoidal or transient signals with rapidly time varying performances. Target information processing for impulse signals is like determining the characteristics of a system from its impulse response [1]. UWB radar operates

simultaneously over a very large bandwidth and the antenna parameters must refer to simultaneous performance over the whole of the bandwidth. So conventional parameters such as frequency domain pattern, gain, etc. are not adequate for UWB antenna .In order to get the impulse response or transient characteristics of the antenna we decided to upgrade our current frequency domain planar near field measurement system to realize time-domain measurement for UWB antennas.

The time-domain technique has many unique advantages over the conventional frequency domain methods, especially for broadband and non-ideal environment measurements. Time domain gating to filter the multiple reflections gives a substantial improvement in measurement accuracy. In addition, Hansen had shown that the scan plane truncation error can be removed by time gating [3].

## 2.0 Time Domain Measurement System Setup

A typical far field time domain measurement system in IRCTR (International Research Center for Telecommunications-transmission and Radar) uses the short time pulses (for example 50 ps) as the UWB excitation signal and sampling oscilloscope as the time domain receiver [2]. This kind of UWB excitation signal is not suitable for the active SAR antenna measurement because: 1) In order to get large absolute bandwidth, SAR antennas commonly operate in X-band or higher frequency .For short time pulses, the pulse energy is distributed over a large number of frequency components, and the resulting reduction of S/N ratio results in a low measurement accuracy at higher frequencies. 2) The T/R module can not operate because the drive power is very low at each frequency components. To solve the above problems the true UWB radar signals such as LFM and phase coded signals are adapted as the excitation signals .As for the oscilloscope, we chose a Lecory SDA 11000 which is a real-time oscilloscope with up to 40 Gsa/s sample rate and 11GHz bandwidth. The N6030A is a wideband arbitrary waveform generator (AWG) that can create high-resolution waveforms for radar, satellite and frequency agile communication systems. Each channel of the N6030A operates at 1.25 GS/s and features 15 bits of vertical resolution.

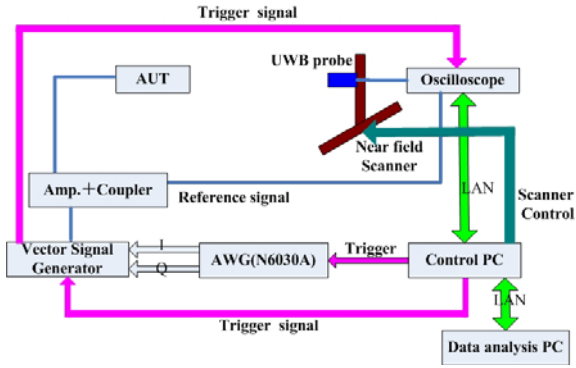


**Figure 1. TD-PNF(time domain planar near field) measurement system setup for UWB antennas, the complex UWB exciting signal is generated by AWG and vector signal generator**

The following are the detail steps needed for TD-PNF measurement: 1) Move the sampling probe (UWB antenna element) along X, Y axis in the scanning plane. When the probe moves to the grid sampling points, the control computer triggers the source (AWG generates the arbitrary wideband external I/Q signals to modulate the vector signal generator.) to send a pulse. 2) The signal comes from wideband coupler's direct output port excites the AUT, at the same time coupling port's signal is sent to oscilloscope for input waveform distortion monitor and compensation. The signal can also be generated by radar if active antenna is measured. 3) The control computer triggers the oscilloscope receive the time-domain signal. The time delay caused by distance between transmitter and receiver antennas along with cables must be considered to synchronize the source and the oscilloscope. 4) Use the frequency-domain or direct time domain computation schema [4] to realize the transformation from near field to far field pattern.

### 3.0 Simulation of the Ku-band standard gain horn under TD-PNF measurement

#### 3.1 The Methods of Simulation

The first AUT we used is Ku band standard gain horn with frequency operating range of 13-18 GHz. The excitation signal adapted is Gauss pulse with carrier. During the practical time-domain near field measurement the time-domain near field data is obtained by measuring the time waveform at discrete grid points on a finite scan plane. The FDTD simulation soft can calculate the far field pattern and the E-field at arbitrary positions and arbitrary time [3]. So we calculated the E-field of  $M \times N$  points in a fictitious plane just as the actual near field sampling signals, then use near field to far field transform program to calculate the antenna radiation pattern. The only difference from the actual measurement is that the sampling probe in the software is an ideal isotropic

antenna so we adapt non-probe compensation formula to realize near field to far field transform.

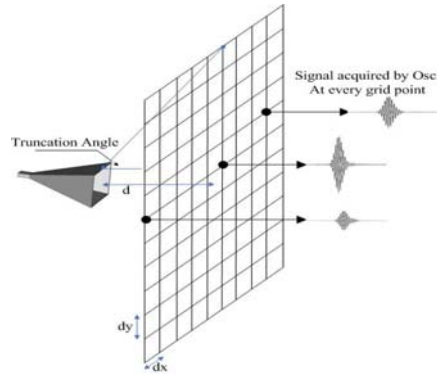


**Figure 2. Standard gain horn under TD-PNF, where  $dx$  and  $dy$  are the sampling spaces. Time-domain waveforms are sampled using oscilloscope at every grid point during measurement.**

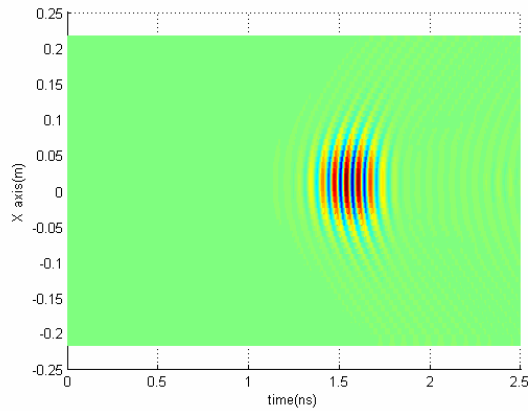


**Figure 3. Calculated probe's output waveforms along x-axis( $y=0$ ) using FDTD to simulate the oscilloscope's sampling signals**

There are five kinds of computation schemes (correspond to different colors in the Figure 4) that we adapted to computed the far field patterns. The direct TD (blue) and non-direct (red) FD near to far field transform are the emphases that will be illuminated in the follow. In order to validate the transform program we measured (green) the AUT using FD-PNF. In addition, IFFT of the frequency domain measurement result and varied time gating [5] were used to increase the measurement accuracy (pink). Due to the changing distance between the probe and the antenna under test (AUT) in planar scans, the conventional fixed time gating technique causes problems to remove multiple reflections from the desired AUT response. So we use the variable time gating according to the different probe's positions to remove reflections. The FDTD simulation result (black) of

radiation pattern is based on the integrating electric current and equivalent magnetic current along the six planes of a cube enclosing the antenna [3].

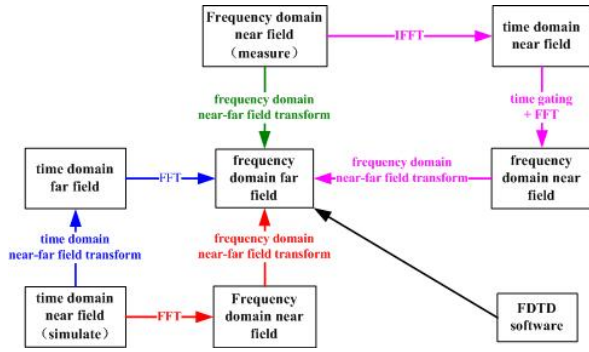


**Figure 4. Five kinds of computation schemes to get the far-field patterns basing on the simulated time domain near field data and measured frequency domain near field data.**

### 3.2 Evaluating the Far Field Using the Direct Time Domain Computation Scheme

The direct time domain formula [4] for the far-field pattern is

$$\bar{F}(\theta, \phi, t) = -\frac{1}{2\pi c} \hat{r} \times \int_{-\infty}^{+\infty} \int_{-\infty}^{+\infty} \hat{z} \times \frac{\partial}{\partial t} \bar{E}(\bar{r}_0, t + \hat{r} \cdot \bar{r}_0 / c) dx_0 dy_0$$

which uses the time-domain near field directly. The formula can be converted the double summation by means of the sampling theorem

$$\bar{F}(\theta, \phi, t) = -\frac{1}{2\pi c} \hat{r} \times \sum_{m=-N_x}^{N_x} \sum_{n=-N_y}^{N_y} \hat{z} \times \frac{\partial}{\partial t} \bar{E}(\bar{r}_{0mn}, t + \hat{r} \cdot \bar{r}_{0mn} / c) \Delta x_0 \Delta y_0$$

For practical application the linear approximation formula is used to the calculate the near field between time samples at times required by the near to far field transforming formula

$$\frac{\partial}{\partial t} \bar{E}(\bar{r}_{0mn}, t) = \frac{1}{\Delta t} \left\{ [(p+1)\Delta t - t] \frac{\partial}{\partial t} \bar{E}(\bar{r}_{0mn}, p\Delta t) + [t - p\Delta t] \frac{\partial}{\partial t} \bar{E}(\bar{r}_{0mn}, (p+1)\Delta t) \right\}$$

where  $\bar{E}(\bar{r}_{0mn}, p\Delta t)$  is the near field at time  $p\Delta t$ . The time derivative  $\frac{\partial}{\partial t}$  can be realized by using “diff” function

provided by MATLAB. The direct TD computation scheme is simpler and easier to program. Furthermore, it has the ability to calculate the far field pattern at early times from near-filed measurements taken at early times only. This is a distinct advantage over FD scheme because sampling the near field at early times not only

can save the test time but also overcome the restriction of the oscilloscope’s deep memory.

### 3.3 Evaluating the Far Field Using the Non-Direct frequency Domain Computation Scheme

First of all, use the Fourier transform to calculate the frequency-domain output of the probe from the time-domain output. Then use the frequency-domain non probe-corrected formulas to calculate the frequency domain far field. At last, use the inverse Fourier transform to calculate the time-domain far field from frequency-domain far field [4]. The core of the frequency domain near field to far field transform is FFT, which express the relation between antenna aperture field and far field. The program language used is Matlab, which provides fast Fourier transform (FFT) function to realize Fourier transform.

### 3.4 Result Analysis

Figure 5 shows the comparison of the measurement result and the simulation result. The measurement result is acquired using NSI PNF test system with HP 85301B RF system.

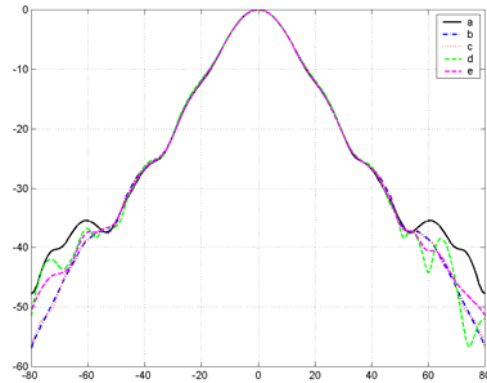


**Figure 5. Comparison of the Ku band horn radiation pattern using different computation scheme: a. FDTD soft solution (black solid) b. Direct TD near-far field transform using simulated TD data (blue dashed and dotted) c. FD near-far field transform using simulated TD data (red dotted) d. FD near-far field transform using measured FD data (green dashed) e. FD near-far field transform with time gating to remove reflections using measured FD data (pink dashed)**

From Figure 5, we note that the TD (line b) and FD (line c) computation schemes get almost the same results, Zoom in the figure you can find that there are some differences between the measured result and the simulation result especially in the 20-30degree region. This error is not resulted from the near field truncation error, which only influence the pattern beyond truncation

angle. We then use the varied time gating to remove the environment influence. After the time gating filter the difference decreased obviously and a good agreement between the two results is achieved in the  $\pm 55$  degree region.

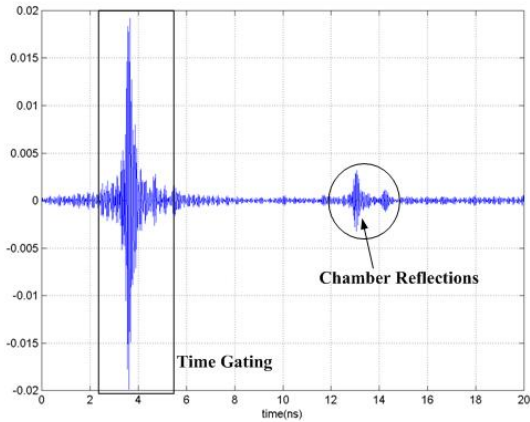


**Figure 6. Time domain near field waveform derived from sweep frequency near field data using IFFT. Time gating was used to remove reflections.**

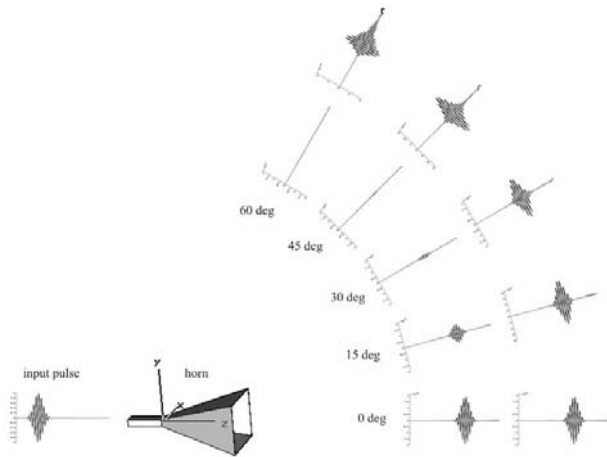


**Figure7. Time domain far field of the horn excited by Gauss pulse with carrier**

Figure 7 is the FDTD simulation results of the far field time domain pattern. We only give the waveforms in five typical directions. The Y axis of each subplot in the inner arc-shaped figure has the same maximum amplitude. The peak amplitude of radiated waveform in each direction embodies the directivity of the AUT. Then we zoom into the subplots to get the detail of the waveforms. From the outer arc-shaped figure we note that the antenna has less waveform distortion in the boresight direction than in the off boresight direction especially great than 30 degree. The fidelity of the antenna's response is the maximum normalized cross-correlation between the incident field

and the received waveform which is a parameter to characterize the UWB antennas [6]. The fidelity is a function of angle off boresight and input waveform for each antenna. As for this AUT the fidelity decreased with the angle (less than 60 degree) off the boresight. But in the back lobe direction the fidelity increases because of the large back lobe caused by horn edges' diffraction.

#### 4.0 TD-PNF Simulation of the Phased Array of Open-ended Waveguide Antennas

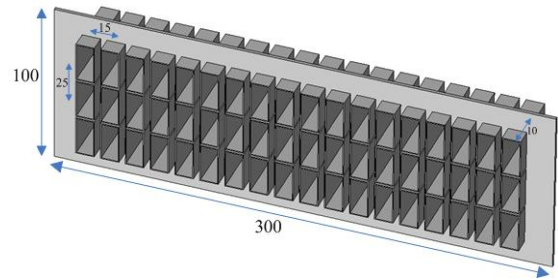


**Figure 8. Model of the waveguide array**

The second antenna used in the simulation is a waveguide array, antenna element is X-band waveguide with  $a=22.86\text{mm}$  and  $b=10.16\text{mm}$ . The space between adjacent elements along narrow side is 15mm, while the space along wide side is 25mm. The amplitude taper satisfy  $-25\text{db}$  Taylor and desired scan angle is set to  $-25\text{degree}$ . In order to achieve higher gain and eliminate the large back lobe, we add a metal reflector behind the waveguide aperture. When adjusting the position of the reflector we found that the VSWR is sensitive to the position of the reflector, and the final optimum distance is 10mm.

LFM is a kind of widely used UWB signal in the SAR, so we choose it as the excitation signal. The frequency operating range is 9.5-12.5GHz. The expression of the LFM signal is

$$s_{\text{LFM}}(t) = A \text{rect}\left(\frac{t}{\tau}\right) e^{j2\pi(f_0 t + \frac{1}{2} u t^2)}$$

where  $A=1$ ,  $\tau = 20\text{ns}$ ,  $f_0 = 9.5\text{GHz}$ ,  $u$  is the chirp slope  $u = B / \tau = 1.5 \times 10^7$ . Under these conditions,  $\tau B = 60 \geq 1$  which makes the pulse compression ratio is large enough to satisfy that 95 percent of the signal power is confined in the frequency band.

For large antennas such as high gain phased array, FD near-far field transform computation takes less time to compute the full 3-D pattern than direct TD computation scheme. So we adapted FD computation scheme in this example.

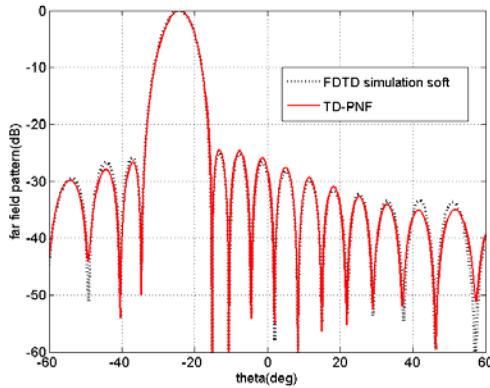


**Figure 9. Comparison of the TD-PNF calculated result (red solid) to FDTD soft result (blue dotted) for the 18 ×3 waveguide array (frequency :9.8GHz)**

Figure 9 shows that the difference is about 2dB at -35dB level. The reason is maybe that the method of FDTD soft calculating of the antenna pattern is to integrate electric current and equivalent magnetic current along the six planes of a cube enclosing the antenna while TD-PNF uses FFT to get the far field pattern.

### 5.0 Summary

Combining the CEM (computational electromagnetics) and the near field to far field transform we simulate the TD-PNF measurements of a standard gain horn and a rectangular waveguide array. The short pulse is extended to the complex UWB signals such as LFM, which is the real radar signal that will be generated by the AWG of the measurement system. The results of the simulation are found to be in close agreement with those derived by FD-PNF measurements. In addition, the TD method has, in principle, distinct advantages over FD methods, for it can provide antenna's transient pattern and impulse response which are important for UWB antenna design and analysis besides higher efficiency, de-noise, or environment diagnosis. So time domain near field measurement technique will find widespread uses in wideband antenna and RCS measurement in the future.

### 6.0 REFERENCES

- [1] James D. Taylor "Introduction to UWB radar systems" CRC press 1995.
- [2] R.V. de Jongh, M. Hajian, L.P. Ligthart, 'Antenna Time-Domain Measurement Techniques', IEEE Antennas and Propagation Magazine, Vol. 39, no.5, pp. 7-12, October 1997.
- [3] Dennis M. Sullivan "Electromagnetic simulation using the FDTD method" IEEE press, 2000.

- [4] T. B. Hansen and A. D. Yaghjian, "Planar near-field scanning in the time-domain. Part 2: Sampling theorems and computation schemes," IEEE Trans. Antennas Propagat. Vol. Ap-42, no.9, pp. 1292-1300, September 1994.

- [5] Yong Zhu "Varied Windows for Time Domain Antenna Near Field Measurement", AMTA 2004.

- [6] Oliver E. Allen, David A. Hill, and Arthur R. Ondrejka, "Time-Domain Antenna Characterizations," IEEE Trans. on Electromagnetic Compatibility, Vol. 35, No. 3, August 1993.